Sādhanā (2020)45:223
https://doi.org/10.1007/s12046-020-01466-3

Flow reversal prediction of a single-phase square natural circulation loop using symbolic time series analysis

RITABRATA SAHA*, KOUSHIK GHOSH, ACHINTYA MUKHOPADHYAY and SWARNENDU SEN

Department of Mechanical Engineering, Jadavpur University, Kolkata 700032, India
e-mail: saha_ritabrata@yahoo.com

MS received 13 April 2018; revised 3 May 2019; accepted 6 June 2019

Abstract. In the field of thermal engineering, one of the biggest concerns is the cooling of heat producing systems. For this purpose, today's world is encouraging to use such cooling systems which are free from any active components (passive systems) for its high reliability and compact size. For this reason, to establish cooling by transferring heat from one place (source) to another (sink) passive system like natural circulation loop (NCL) is highly used. Fluid flow dynamics of the NCL is changing with the increase in heater power which is used as the source for the simulation. We found steady flow dynamics for the comparatively low power of heat, and with the rise in the power first, we saw the oscillatory flow dynamics and then found flow reversal characteristics. This paper presents a novel strategy for the early prediction of flow reversal phenomenon in NCL using symbolic analysis of time series data. This time series data is found from the numerical simulation, and for the proper study, we are considering data after the initial transient part is overcome. Total time series data is transformed into a symbol string by partitioning into a finite number of specified symbolised groups. The state probability vector is calculated based on the number of occurrences of each symbol group. Present work is a single-phase study, and according to our geometry, we can provide a maximum 800 W heater power to stay in the single-phase. Therefore, for the early prediction of flow reversal in NCL, state probability vector evaluated at 800 W heater power which is the most undesirable state (chaotic data), and this is considered as the reference vector. The difference of the reference state vector from the current state vector is used as a parameter for early detection of flow reversal. It can be observed from the results that this difference changes significantly when the system is sufficiently away from the flow reversal.

Keywords. Natural circulation loop; flow reversal; instability; symbolic time series analysis.

1. Introduction

In the field of thermal engineering, one of the biggest concerns is the cooling of heat producing systems. For this purpose, today's world is encouraging to use such cooling systems which are free from any active components (passive systems) for its high reliability and compact size. For this reason, as a cooling system, natural circulation loop (NCL) has been used in various energy systems like electrical machine rotor cooling, solar water heater systems, geothermal energy systems and nuclear power plants, etc. [1]. Heat removal is performed by the circulation of the fluid present in the NCL. Fluid circulation is established due to the absorption of heat from a heat source and transporting it to a heat sink without the help of any pumping device, and this is the main advantage of natural circulation over forced circulation. Due to the absence of mechanical components which can fail to perform, NCL added more reliability to the systems. In NCL, the direction of fluid flow is determined by the temperature difference present between different points of the loop, on which the buoyancy force depends.

The occurrence of unstable dynamical behaviours is one of the significant problems in NCL, which are produced due to the temperature oscillations. The growth of these oscillations is not desirable for any system as it may cause changes in the relative magnitudes of temperature in the two limbs in an oscillating fashion and produce a periodic inversion of the flow direction. The occurrence of this flow reversal may affect the heat removal from the thermal source and may cause failure of the whole system. This problem motivated the researchers to identify the flow dynamics of NCL accurately over the past few years. This

This paper is a revised and expanded version of an article presented in "First International Conference on Mechanical Engineering" held at 'Jadavpur University', Kolkata, India during January 4–6, 2018 (INCOM-2018).

*For correspondence

Published online: 02 September 2020

identification will help to design an appropriate control strategy to mitigate the instabilities associated with the NCL and to perform the stable operation of the systems which depend on NCL. For the practical control strategy, it is essential to predict early for which operating conditions flow reversal phenomenon is about to begin.

Compared to two-phase NCLs single-phase NCLs are more stable. Therefore, many engineering sectors are using single-phase NCLs to transfer heat from one place to another. Accordingly, in the last few decades, researchers are putting lots of effort to study the flow dynamics and controlling the instability associated with the single-phase NCL. Experimental and numerical investigations have been carried out by Vijayan *et al* [2] to find out the stable regime from the flow dynamics of the NCL. From the experimental data, it was found that we can divide the flow dynamics into three categories whereas numerically flow dynamics can be divided into two groups. They also found a conditionally stable region near the stability threshold. Fichera *et al* [3] performed experiments to observe the dynamic stability of two different geometrical rectangular loops. They found a substantial difference in flow dynamics due to the change in geometry. But for both the geometry with the increase in heater power flow dynamics was changing from steady to chaotic through periodic oscillation. Luzzi *et al* [4] studied fluid flow dynamics using a stability map approach. For this, they were using experimental data along with semi-analytical and numerical models. Mathematical analysis and linear stability have been carried out for a rectangular NCL by Nayak *et al* [5] for the stability characterization of the loop fluid flow. They were using Nyquist stability criterion, to observe the stable, unstable and neutrally stable points from the time series data of temperature oscillations and flow amplitude. Using the stability mapping, comparison of these two results are executed. Cammarata *et al* [6] conducted experiments on NCL. Using this experimental result nonlinear analysis was carried out to study the loop fluid flow dynamics. Phase Space Reconstruction, Singular Value Decomposition and Average Mutual Information techniques are being used as the nonlinear analysis tools to observe the flow dynamics. Two-dimensional numerical modelling has been done by Desrayaud *et al* [7] to investigate the flow dynamics for a rectangular NCL. They found that there was a significant effect of the Rayleigh number on the flow characteristics.

Different experiments are executed by Vijayan *et al* [8] to study the flow dynamics. They also performed numerical analysis by the computer code ATHLET to observe the effect of the loop diameter and power level on the flow dynamics. They found that with the increase in loop diameter and power level instability present in the flow dynamics increases. To simulate the flow pattern of a single phase NCL Mousavian *et al* [9] used the RELAP5 system code. After that with the help of stability mapping and Nyquist stability criterion they have performed the stability analysis. Pini *et al* [10] observed the effect of internal heat generation along with heat exchange on the flow stability using RELAP5 and CFD code. They found that in the presence of internal heat generation fluid flow stability gets increased. Numerical investigations have been carried out by Ridouane *et al* [11] for the fluid circulation in unstable convection regime of a toroidal NCL. They observed that with the increasing Rayleigh number, the occurrence of flow reversal was increasing. For each of the flow regime, they saw the local heat flux distributions, isotherms and streamlines. Jiang *et al* [12] studied flow stability for a copper toroidal thermosyphon, experimentally and numerically. They found that copper torus is more stable than usual glass torus. Maiani *et al* [13] performed a stability analysis by stability mapping using an analytical model of a single-phase thermosyphon loop. Using experiments and numerical analysis fluid flow dynamics have been investigated for an annular thermosyphon by Desrayaud *et al* [14].

Steady state analysis and linear stability analysis for the supercritical water natural circulation loop (SCWNCL) have been performed using a computer code SUCLIN by Sharma *et al* [15]. Also, they have studied the parametric effect. For an NCL which is filled with supercritical CO_2 numerical investigations have been performed by Chen *et al* [16]. They investigated the flow transitions and instabilities associated with the loop fluid circulation. To calculate the stabilities of the system temperature-sensitive physical properties are being used. From their investigations, it was observed that because of the presence of supercritical CO_2 as loop fluid, fluid flow characteristics change from unstable flow reversal behaviour to stable one directional flow pattern with the increase in source temperature. From the experiments performed by the Nayak *et al* [17], it was found that using water with a small concentration of Al_2O_3 nano-fluid suspended in it flow instability associated with the NCL can be reduced significantly. But if we increase the intensity of Al_2O_3 into the water then flow instability again increased. Zboray *et al* [18] performed experiments on two-phase natural circulation loop under different system pressure condition. They found that with the increase in heater power, the flow became chaotic through Hopf bifurcation and period-doubling. Satoh *et al* [19] numerically studied the effects of multiple tubes on the stability of the toroidal NCL. They found five different flow regimes with the increase in heat flux because of the multiple tubes. Flow dynamics of these regimes were observed by the phase space attractors.

The objective of the present work is an early prediction of flow reversal phenomenon. Numerical simulations have been carried out using MATLAB based Simulink model which was developed in our previous works [20, 21]. With the gradual increment of the operating power flow dynamics of the NCL is changing from steady-state characteristics to flow reversal characteristics through the oscillatory region. From the characterization of flow dynamics, we observed that oscillatory flow is purely periodic and flow reversal is chaotic in nature. Now as the

chaotic behaviour is not suitable for any system, therefore, we need the early prediction of flow reversal so that we can trigger the control mechanism correctly. Symbolic time series analysis (STSA) [22–25] provides an elegant way for this purpose.

2. Numerical modeling

Numerical model and the geometry (figure 1), applied here, was explained in detail in our previous paper [20, 21]. Governing equations of mass, momentum and energy for the loop fluid are presented in Eqs.(1) to (3), respectively. The energy equations for coolant and tube wall are given in Eqs. (4) and (5), respectively. These equations are identical to our earlier works [20, 21], therefore repeated explanations are being ignored of this equations for the compactness of the paper.

$$\frac{\partial \rho_f}{\partial t} + \frac{\partial}{\partial z}\left((\rho v)_f\right) = 0 \tag{1}$$

$$\frac{d\rho v_f}{dt} L_{loop} = -\frac{f_{in}(\rho v)_f^2}{2\rho_f d_{in}} L_{loop} + \oint \rho_0 g \beta_{av}(T_f - T_{ref}) dz \tag{2}$$

$$\frac{\partial}{\partial t}\left(\rho_f C_p T_f\right) + \frac{\partial}{\partial z}\left((\rho v)_f C_p T_f\right) = \frac{\partial}{\partial z}\left(k_f \frac{\partial T_f}{\partial z}\right) - \frac{4h_i(T_f - T_w)}{d_{in}} \tag{3}$$

$$\frac{\partial}{\partial t}\left(\rho_{ex} C_{pex} T_{ex}\right) + \frac{\partial}{\partial z}\left((\rho v)_{ex} C_{pex} T_{ex}\right) = \frac{\partial}{\partial z}\left(k_{ex} \frac{\partial T_{ex}}{\partial z}\right) + \frac{h_{ex} A_0 (T_w - T_{ex})}{V_{ex}} \tag{4}$$

The heat conduction equation for tube wall is

$$\frac{\partial}{\partial t}\left(\rho_w C_{pw} T_w\right) = \frac{\partial}{\partial z}\left(k_w \frac{\partial T_w}{\partial z}\right) + \frac{h_i A_i (T_f - T_w)}{V_w} - \frac{(h_0 + h_r) A_0 (T_w - T_a)}{V_w} + \frac{\dot{Q}}{V_w} \tag{5}$$

For the numerical simulation, based on the Simulink model above governing equations were being solved and for this purpose, several closure relations were implemented which are identical to our earlier works [20, 21]. Therefore, we have not repeated the closure relations here for the compactness of the paper.

2.1 *Symbolic Time Series Analysis (STSA)*

The Symbolic time series analysis (STSA) [22–25] reveal the behaviour of nonlinear dynamical systems from the time series data by symbolization and state machine construction. After the symbolization, the state probability vectors are produced. In STSA the generation of a

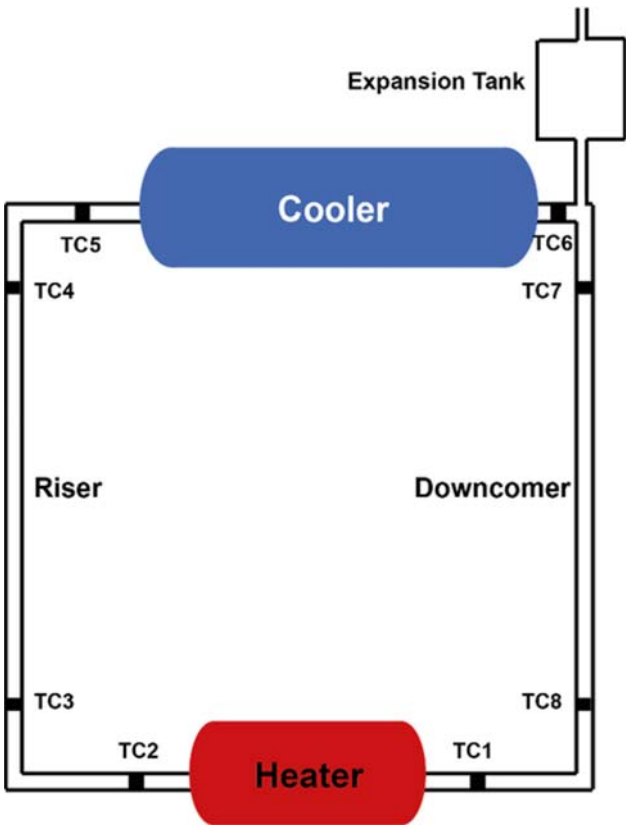

Figure 1. Schematic diagram of a square natural circulation loop [20, 21].

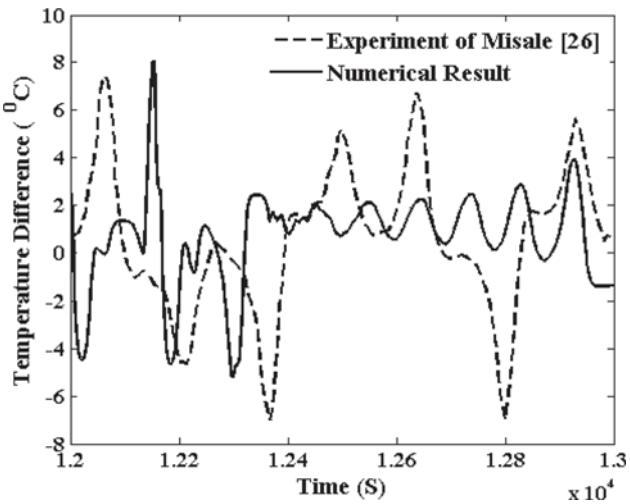

Figure 2. Variation of temperature difference with time at 500 W.

Table 1. Comparison of temperature difference with the result of Misale [26].

Temperature Difference	Experiment of Misale [26]	Numerical Result
Variation Range	−6.9°C to 7.4°C	−7.8°C to 5.0°C
Average Absolute Value	0.63°C	0.66°C

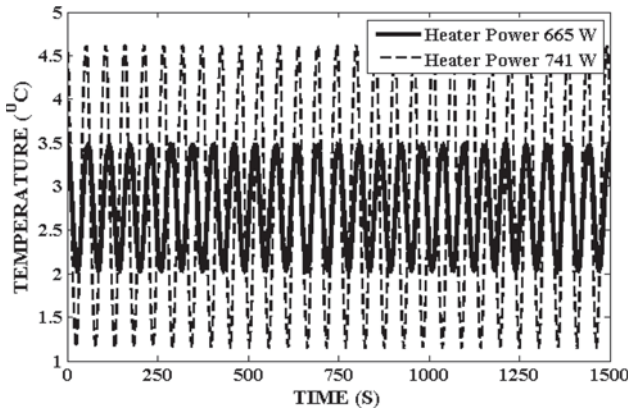

Figure 3. Variation of temperature difference with time at 665 W and 741 W.

proper symbol string is essential. Total time series data is partitioned into a finite number of non-overlapping contiguous cells to create symbolic time series in the present application. This time series data which is used here is found from the numerical simulation, and for the proper study, we are considering data after the initial transient part is overcome. A unique symbol has been assigned to every instantaneous value of the measured variable that dips in that partitioned region. Thus, the discrete time series data of the state variable is modified to a symbol string. For the generation of the symbol string, the time series data can be divided with the help of uniform partitioning or maximum entropy partitioning. In the present work, we are using maximum entropy partitioning approach, so that occurrence probability (i.e., number of data points in each group) will be equal for each group in the reference state. This maximizes the information entropy *H(n)* which can be expressed as:

$$H(n) = -\sum_{i=1}^{i=n} p_i \log p_i$$

Where p_i denotes the probability of occurrence of a symbol s_i in the symbol string. Symbolic time series have been generated in this work using simple partitioning (SP), where the time series data are being applied directly to the partitioning. The word size D is taken as 1 and, hence, the number of possible states becomes equal to the number of symbols. If p^k is the reference state probability vector and p^l is the current state probability vector, then a scalar anomaly-measure d(p^k, p^l) which is the angular distance (M) between current probability vector p^l from the reference probability vector p^k can be used for the prediction of flow reversal.

$$M = \cos^{-1} \frac{\langle p^k, p^l \rangle}{\|p^k\| \|p^l\|}$$

where $< p^k,\ p^l >$ denote the inner product of the state probability vectors p^k & p^l, and $\| p \|$ indicates the Euclidean norm of the vector p.

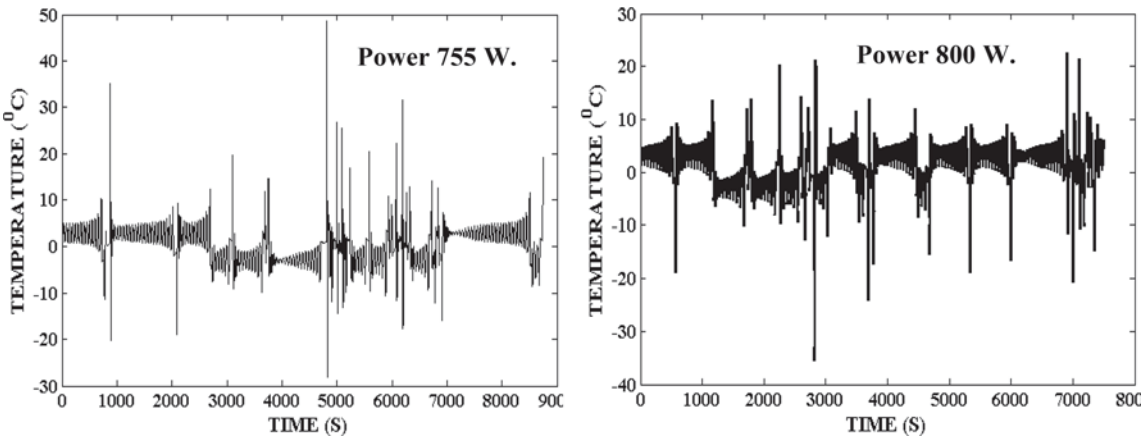

Figure 4. Variation of temperature difference with time at 755 W and 800 W.

3. Validation

A model validation analysis has been performed to assess the accuracy and reliability of our MATLAB based SIMULINK model. The present model is validated with the experimental work of Misale [26]. They performed experiments at different heater power levels. With their experimental configuration, we performed numerical simulation using our numerical model, and the comparison of these two results is shown in figure 2. This comparison is for 500 W heater power. The present work is qualitatively matched with that of Misale [26]. Here, it is noteworthy that the time series data of the two studies are not matching precisely because of the inherent nonlinearity of the problem. However, the temperature variation range and the average value of temperature found from the present work are in good agreement with that of Misale [26], as shown in table 1.

Also, the grid and time independence study is supplied in our previous work [21] and for the compactness of the paper, is not reported here again.

4. Results and discussions

Fluid flow dynamics obtained from the numerically simulated time series data can be divided into three categories. For operating power below 625 W, it shows steady-state behaviour, for 625 W to 742 W it shows periodic oscillation, and for above 742 W, it shows flow reversal phenomenon which is chaotic in nature [27, 28]. For the proper

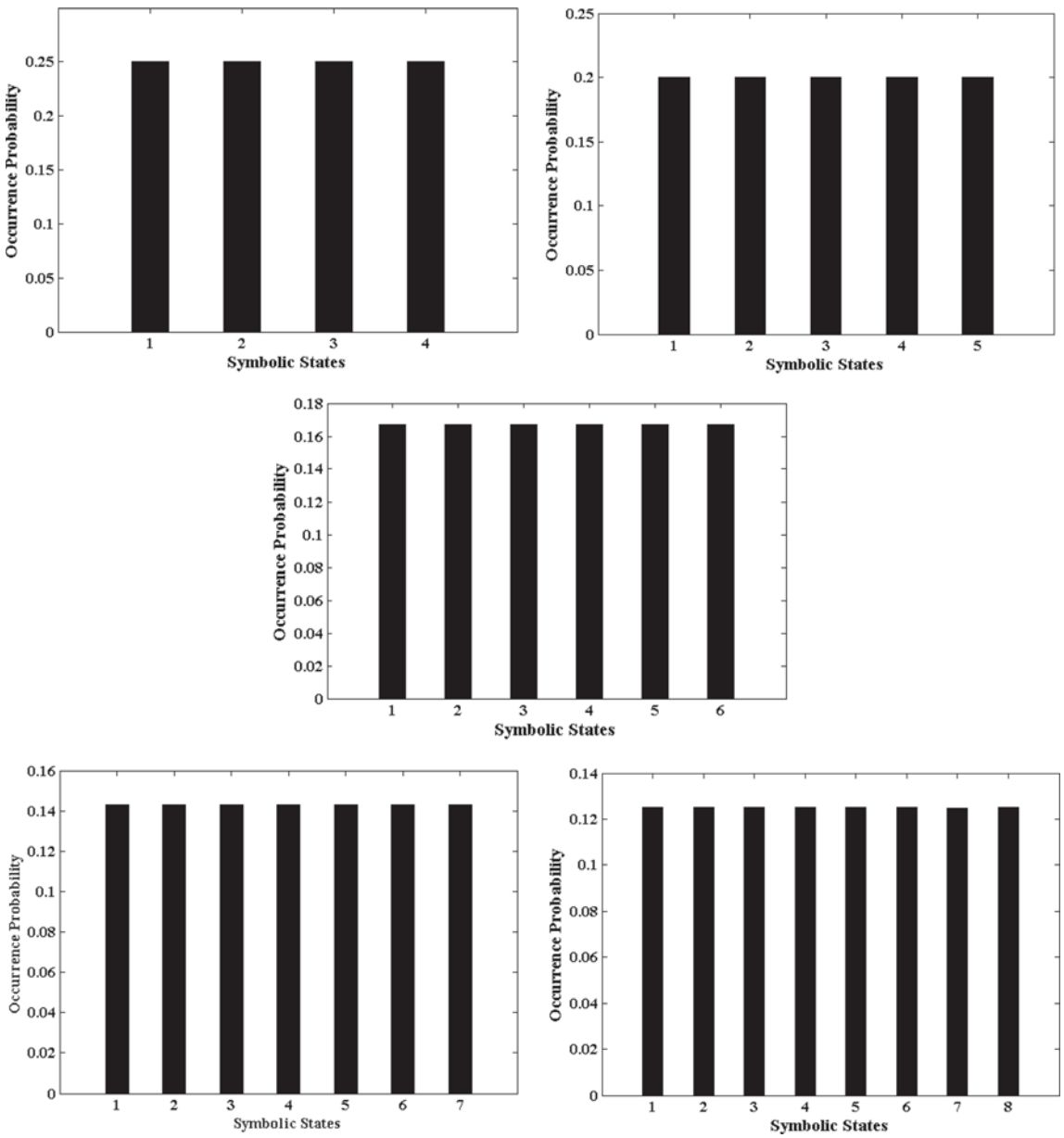

Figure 5. Symbolic state histogram at 800 W for a different number of groups (Reference State).

analysis of the time series data, we are considering the data after the initial transient part is overcome. In an NCL driving force for the fluid flow comes from the temperature difference between its two vertical arms - the riser (having a higher temperature) and the down-comer (having a lower temperature). We are considering the middle points of the two vertical arms for calculating the temperature difference. The temperature difference between these two vertical arms creates a density difference, and this, in turn, produces the fluid flow by equilibration of the buoyancy, friction and gravitational forces.

For the heater power of 665 W and 741 W variation of temperature difference with time is shown in figure 3. Zero time for figure 3 specifies that time from where we start the observation after the transient. From figure, it can be found that with the increase in heater power oscillation amplitude increases. For heater power of 665 W, the oscillation amplitude (the difference between the maximum and minimum temperature difference) of the temperature difference is about 1.5°C while for the heater power of 741 W, the oscillation amplitude increases to about 3.3°C. These oscillations are purely periodic in nature [27, 28].

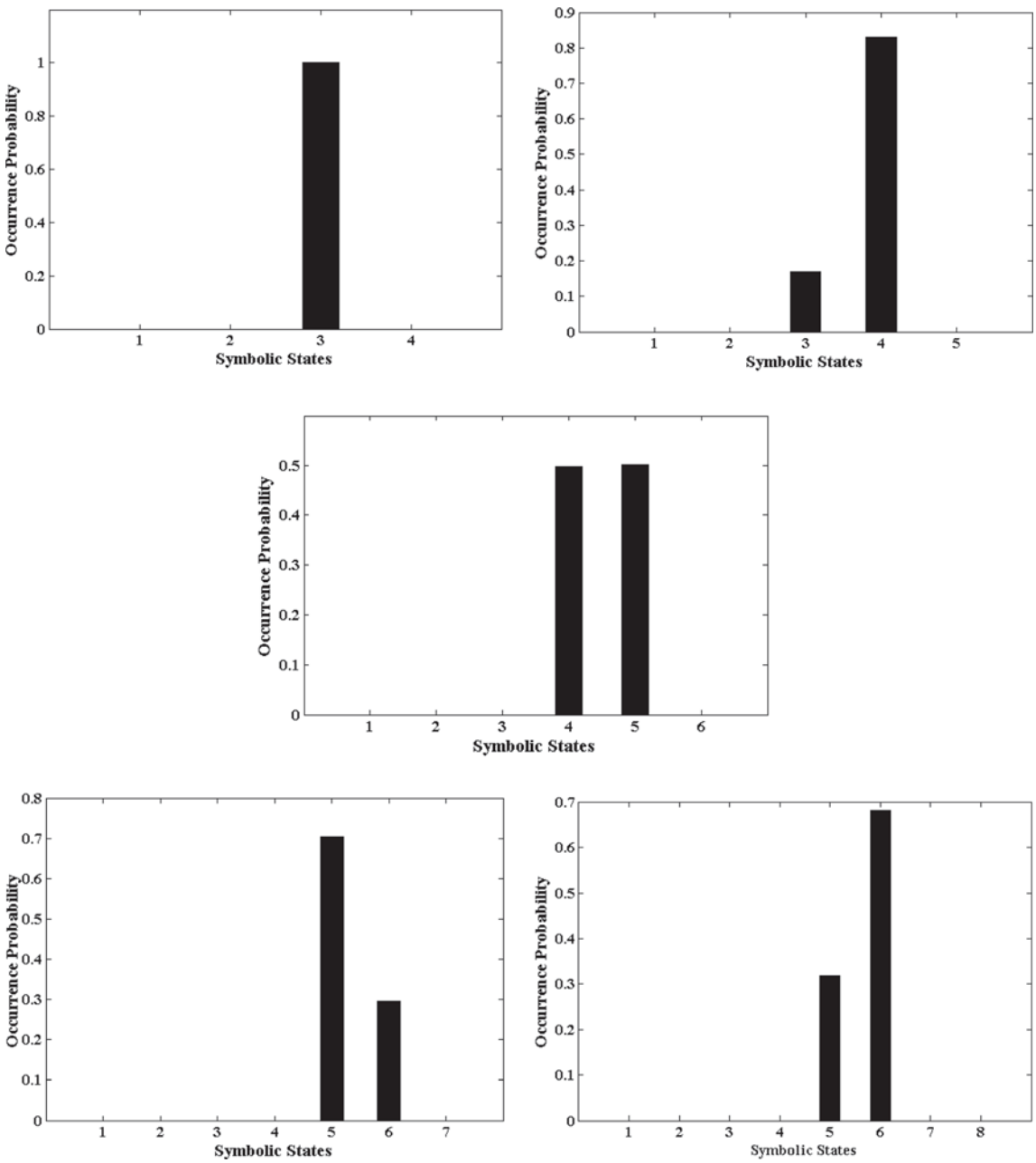

Figure 6. Symbolic state histogram at 665 W for a different number of groups.

For heater power of 755 W and 800 W, the variation of temperature difference with time is shown in figure 4. Zero time for figure 4 specifies that time from where we start the observation after the transient. From the figure, it can be found that the variation of temperature difference shows flow reversal characteristics. The frequency of occurrence of flow reversal increases with increasing heater power. From the nonlinear analysis, it is found that this flow reversal phenomenon is chaotic in nature [27, 28]. NCLs are used in various power plants as a heat removal device and therefore for the safety of the plants flow reversal is an undesirable phenomenon. Due to this, we must avoid flow reversal conditions. Consequently, we need the early prediction of flow reversal so that we can trigger the control mechanism correctly.

Figure 5 shows symbolic state histogram at 800 W heater power for a different number of symbolic groups. This is a single-phase study, and according to our geometry, we can provide a maximum 800 W heater power to stay in the single-phase. Therefore, for the early prediction of flow reversal in NCL, we have taken a most undesirable state (chaotic data) which is 800 W heater power state as our reference state. Numerically found temperature difference time series data is used for the symbolic time series

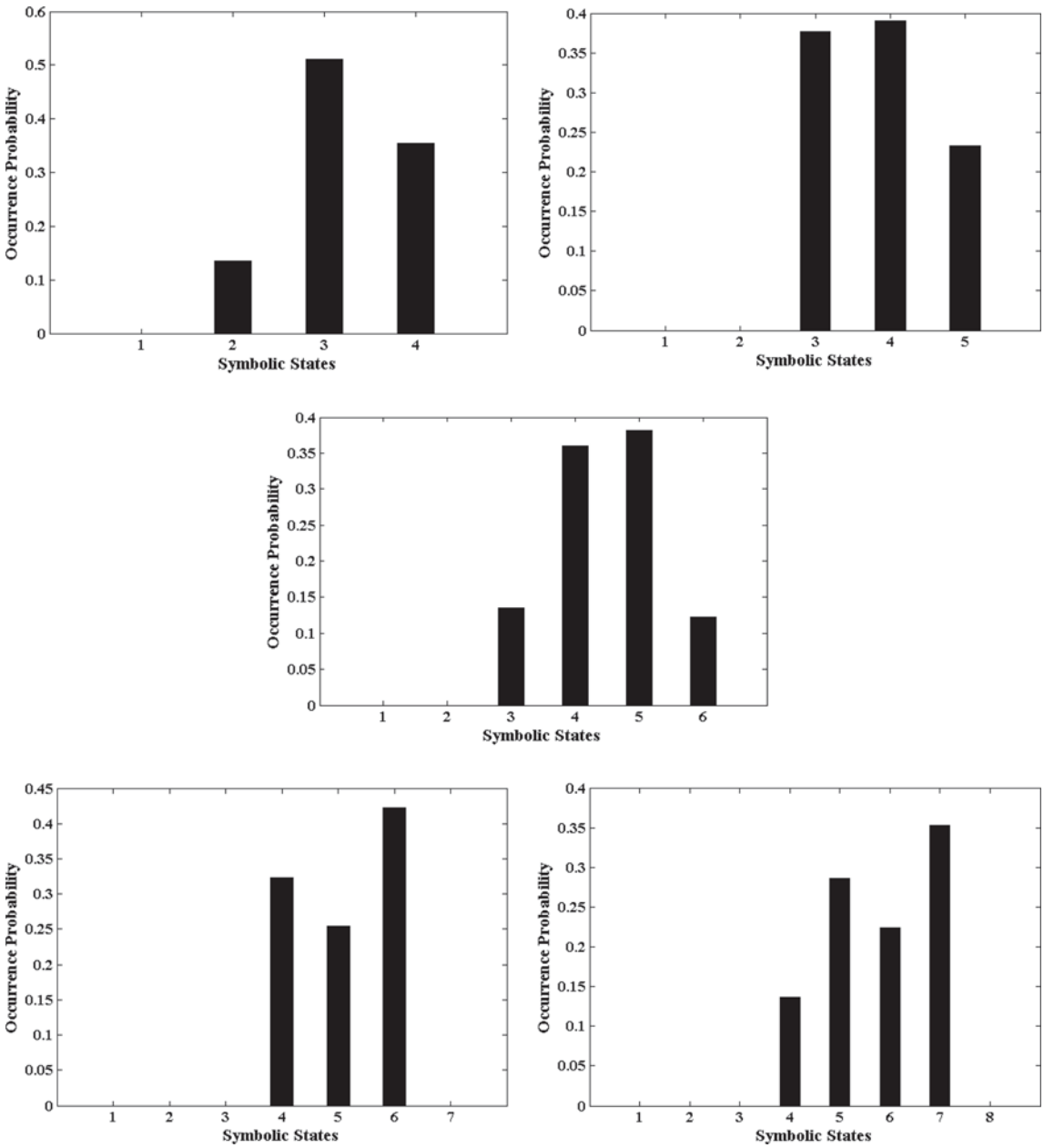

Figure 7. Symbolic state histogram at 741 W for a different number of groups.

analysis. For the proper study, we are considering time series data after the initial transient part is over. Total time series data is partitioned into a different number of groups, and a symbol is assigned to each group. Thus, the time series data is transformed into a symbol string. The state probability vector is calculated based on the number of occurrences of each symbol group for the time series data. For the symbol string generation, time series data was partitioned using maximum entropy partitioning so that each group in reference state has an equal probability as shown in figure 5.

To observe the effect of the number of symbolic groups for case-I we divide total time series data into four number of groups and similarly for case-II five number of groups, for case-III six number of groups, for case-IV seven number of groups and for case-V eight number of groups as shown in figure 5.

Symbolic state histogram with the comparison of respective reference state for heater power 665 W, 741 W and 755 W are shown in figures 6, 7 and 8, respectively. From figures, it can be observed that symbolic state histograms show significant deviation from the respective

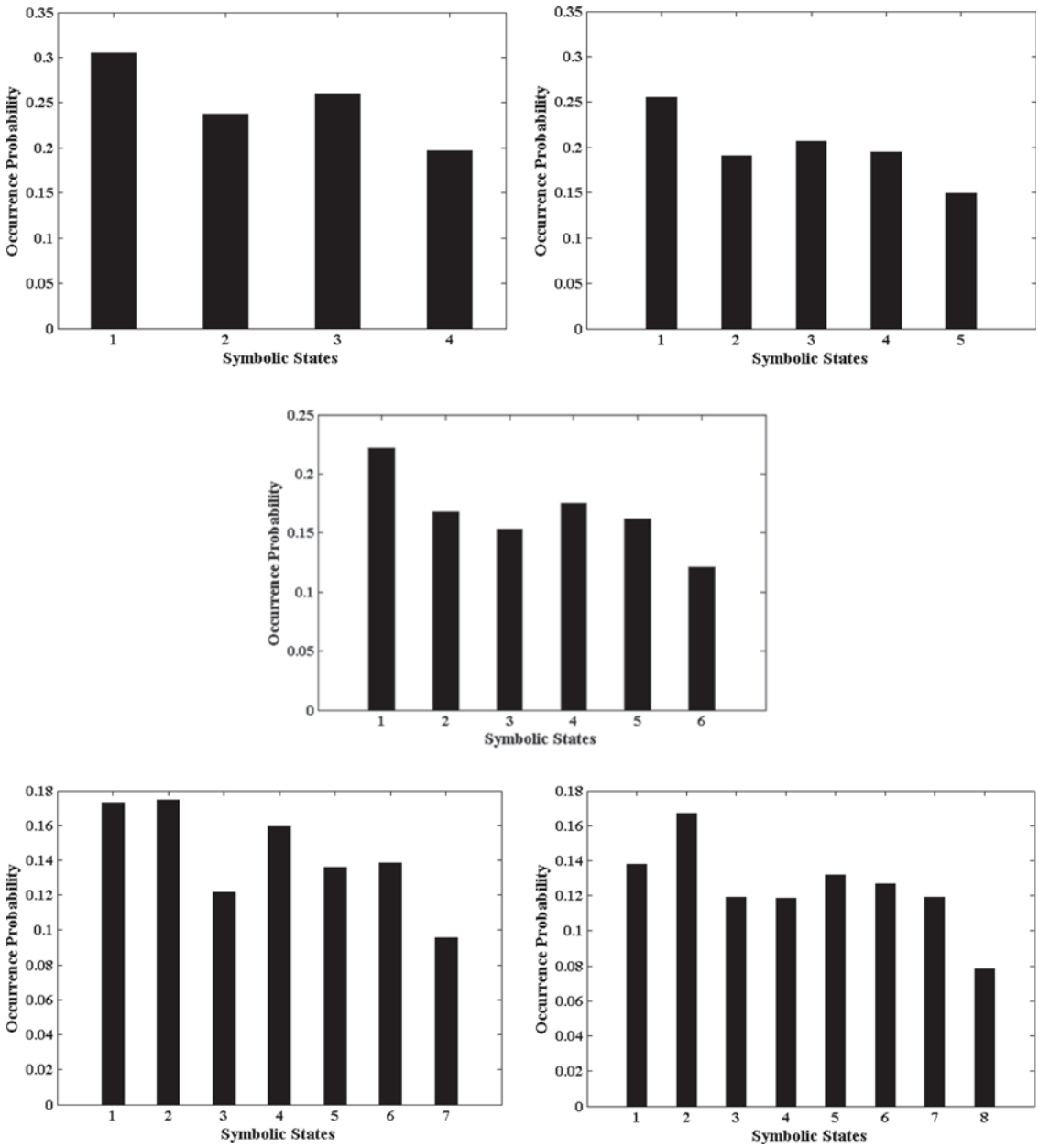

Figure 8. Symbolic state histogram at 755 W for a different number of groups.

reference state when it is in the early periodic regime (figure 6) and when it goes towards a chaotic regime (figure 7) or in the chaotic regime (figure 8) its shows more and more better machine. So, from the symbolic state histogram, we can find how far we are from an undesirable state.

From figure 6 it can be observed that all the data points accumulated in one symbolic state for case-I and for other cases it is divided into two symbolic states in the symbolic state histogram. Also, it can be observed that for case-III all the data points are divided into two symbolic states with almost equal probability.

From figure 7 for all the cases data points are divided into three or four symbolic states which are more towards the respective reference symbolic state histogram as shown in figure 5. But the distribution is much more evenly poised for the case-III.

From figure 8 it can be observed that for all the cases data points are divided into all the symbolic states, and symbolic state histogram is quite like the respective reference symbolic state histogram as shown in figure 5. Therefore, from the figures (figures 6, 7, 8) it can be said that in comparison to all the cases, case-III which is related to the six number of groups shows a better result.

Figure 9 shows a variation of deviation (anomaly measure) with heater power for all the cases. From figure 9 it can be observed that for the periodic regime deviation from the reference state is quite high, and when it comes closer to the chaotic regime, deviation becomes smaller and smaller for all the cases. In the periodic regime deviation from the reference state shows a steady value for the case-III but for all the other cases deviation from the reference state shows fluctuating in nature. However, in close to the chaotic regime deviation from the reference state starts decreasing for all the cases. So, in comparison with all the cases, case-III provide the best result in terms of prediction of the onset of flow reversal.

Figure 10 shows a variation of information entropy with heater power for all the cases. From figure 10 it can be observed that for the periodic regime, information entropy stays at a very low value for all the cases and when the heater power comes close to the chaotic regime, information entropy starts increasing for all the cases, and in the chaotic regime, information entropy stays at a very high value. In the periodic regime information entropy is nearly constant for the case-III but for all the other cases information entropy shows fluctuating in nature. However, in close to the chaotic regime information entropy starts increasing for all the cases. So, in comparison with all the cases, case-III provide the best result in terms of prediction of the onset of flow reversal.

Therefore, from the variation of deviation with heater power as shown in figure 9 and the variation of information entropy with heater power as shown in figure 10 we can observe that for the periodic region only case-III show steady constant value and when we move towards chaotic region deviation starts falling, and information entropy starts increasing. But for the other cases deviation starts falling and information entropy starts increasing way before the chaotic region starts. Therefore, for these cases, we get the wrong intimation about the start of the chaotic region. So, in comparison to all the cases, we can only use case-III for the early prediction of the chaotic region.

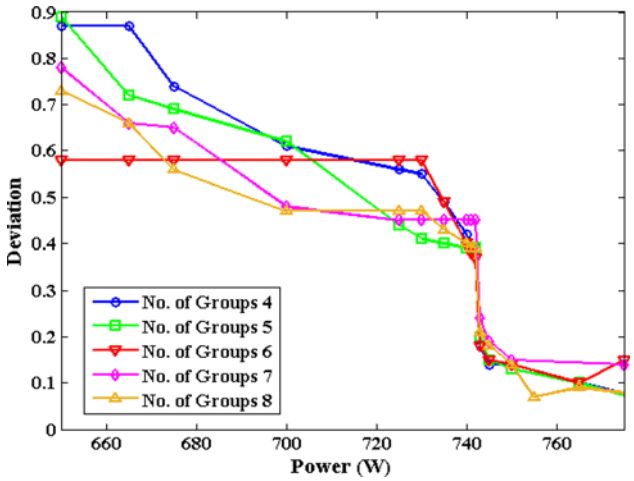

Figure 9. Variation of deviation with heater power for a different number of groups.

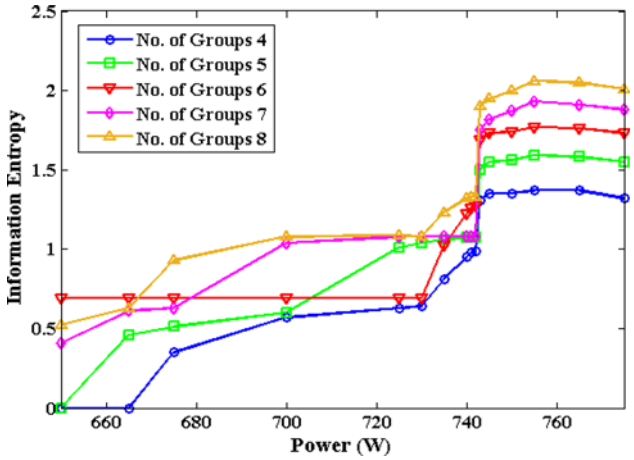

Figure 10. Variation of information entropy with heater power for a different number of groups.

5. Conclusion

Fluid flow dynamics obtained from the numerically simulated time series data can be divided into three categories. For operating power below 625 W., it shows steady-state behaviour, for 625 W. to 742 W. it shows periodic oscillation, and for above 742 W., it shows flow reversal phenomenon which is chaotic in nature. We are using symbolic

time series analysis for early prediction of flow reversal. Numerically found temperature difference time series data is used for the STSA. Total time series data is partitioned into a different number of groups, and a symbol is assigned to each group. The time series data was partitioned for symbol string generation using maximum entropy partitioning. We have taken a most undesirable state (chaotic data) which is 800 W heater power state in single-phase as our reference state. Effect of the number of symbolic groups is being analyzed. For case-I, we divide total time series data into four number of groups and similarly for case-II five number of groups, for case-III six number of groups, for case-IV seven number of groups and for case-V eight number of groups.

From the symbolic state histograms, we found that there is a significant deviation in symbolic states in compare to the respective reference state when time series data belong to the early periodic regime and when it goes towards chaotic regime or in the chaotic regime symbolic state histograms shows more and better machine with the respective reference state histograms. So, from the symbolic state histograms, we can determine how far we are from an undesirable state.

In the periodic regime, deviation from the reference state is quite high, and when it comes closer to the chaotic regime, deviation becomes smaller and smaller for all the cases. Also, in the periodic regime, information entropy stays at a very low value for all the cases, and when the heater power comes close to the chaotic regime, information entropy starts increasing for all the cases, and in the chaotic regime, information entropy stays at a very high value. So, with the help of deviation from the reference state and information entropy, we can predict the flow reversal phenomenon quite early.

In the periodic regime deviation from the reference state and information entropy show a steady value for the case-III but for all the other cases deviation from the reference state and information entropy show fluctuating in nature. However, in close to the chaotic regime deviation from the reference state starts decreasing and information entropy starts increasing for all the cases. So, in comparison with all the cases, case-III provide the best result in terms of prediction of the onset of flow reversal.

Acknowledgement

This paper is a revised and expanded version of an article entitled, "Flow Reversal Prediction of a Single-Phase Square NCL using Symbolic Time Series Analysis", Paper No., "INCOM18-078" presented in "First International Conference on Mechanical Engineering" held at 'Jadavpur University', Kolkata, India during January 4-6, 2018. The first author owes to the University Grants Commission (UGC) for issuing the fellowship under UPE - Phase-II Program.

Nomenclature

A	Area of cross section (m^2)
A_{in}	Internal cross-section area of the loop (m^2)
A_0	External cross-section area of the loop (m^2)
C_p	Specific heat of fluid at constant pressure (J/kg·K)
C_{pw}	Specific heat of wall at constant pressure (J/kg·K)
C_{pex}	Specific heat of coolant at constant pressure (J/kg·K)
d_{in}	Internal loop diameter (mm)
Dz	Change in length (m)
F	Friction factor
Gr	Grashof number
Gr_m	Modified Grashof number $((D^3\rho_f^2\beta_{av}gL_H\dot{Q})/(A\ \mu_f^3\ C_p)$
Gz	Graetz number
Nu	Nusselt number
Pr	Prandtl number
T	Time (Sec)
T_f	Temperature of fluid (°C)
T_w	Loop wall temperature (°C)
T_{ex}	Coolant temperature (°C)
T_{ref}	Reference temperature (°C)
T_a	Ambient temperature (°C)
Ra	Rayleigh number
h_i	Heat transfer coefficient between fluid & wall (W/m^2·K)
h_o	Heat transfer coefficient between wall & ambient (W/m^2·K)
h_{ex}	Heat transfer coefficient between wall & coolant (W/m^2·K)
k_f	Thermal conductivity of fluid (W/m·K)
k_w	Thermal conductivity of wall (W/m·K)
k_{ex}	Thermal conductivity of heat exchanger (W/m·K)
L_{loop}	Total loop length (m)
L_H	Loop height (m)
N_G	Length to diameter ratio (L_{loop} / D)
Re_d	Reynolds number
$\dot{Q}$	Volumetric heat generation (W/m^3)
v_f	Fluid velocity (m/s)
V_w	Wall volume (m^3)
V_{ex}	Heat exchanger fluid volume (m^3)
β_{av}	Thermal volumetric expansion coefficient (K^{-1})
μ_f	Dynamic viscosity of fluid (kg/m·s)
υ	Kinematic viscosity of fluid (m^2/s)
ρ_f	Fluid density (kg/m^3)
ρ_w	Density of wall (kg/m^3)
ρ_{ex}	Coolant density (kg/m^3)

References

[1] Sinha R K and Kakodkar A 2006 Design and development of the AHWR—the Indian thorium fuelled innovative nuclear reactor. *Nucl. Eng. Des*. 236: 683–700

[2] Vijayan P K, Sharma M, Pilkhwal D S, Saha D, Sinha R K, Bhojwani V K and Sane N K 2004 Experimental and numerical investigations on the nature of the unstable oscillatory flow in a single-phase natural circulation loop. In: *XVII National and VI ISHMT/ASME Heat and Mass Transfer Conference*. IGCAR, Kalpakkam

[3] Fichera A, Froghieri M and Pagano A 2001 Comparison of the dynamical behaviour of rectangular natural circulation loops. *J. Process Mech. Eng. Part E*. 4: 273–284

[4] Luzzi L, Misale M, Devia F, Pini A, Cauzzi M T, Fanale F and Cammi A 2017 Assessment of analytical and numerical models on experimental data for the study of single-phase natural circulation dynamics in a vertical loop. *Chem. Eng. Sci.* 162: 262–283

[5] Nayak A K, Vijayan P K, Saha D and Raj V V 1995 Mathematical modelling of the stability characteristics of a natural circulation loop. *Math. Comput. Model*. 22: 77–87

[6] Cammarata G, Fichera A and Pagano A 2000 Nonlinear analysis of a rectangular natural circulation loop. *Int. Commun. Heat Mass Transf.* 27: 1077–1089

[7] Desrayaud G, Fichera A and Lauriat G 2013 Two-dimensional numerical analysis of a rectangular closed-loop thermosiphon. *Appl. Therm. Eng*. 50: 187–196

[8] Vijayan P K, Austregesilo H and Teschendorff V 1995 Simulation of the unstable oscillatory behaviour of single-phase natural circulation with repetitive flow reversals in a rectangular loop using the computer code ATHLET. *Nucl. Eng. Des*. 155: 623–641

[9] Mousavian S K, Misale M, D'Auria F and Salehi M A 2004 Transient and stability analysis in single-phase natural circulation. *Ann. Nucl. Energy* 31: 1177–1198

[10] Pini A, Cammi A and Luzzi L 2016 Analytical and numerical investigation of the heat exchange effect on the dynamic behaviour of natural circulation with internally heated fluids. *Chem. Eng. Sci.* 145: 108–125

[11] Ridouane E H, Danforth C M and Hitt D L 2010 A 2-D numerical study of chaotic flow in a natural convection loop. *Int. J. Heat Mass Transf.* 53: 76–84

[12] Jiang Y Y, Shoji M and Naruse M 2002 Boundary condition effects on the flow stability in a toroidal thermosyphon. *Int. J. Heat Fluid Flow* 23: 81–91

[13] Maiani M, Kruijf W J M D and Ambrosini W 2003 An analytical model for the determination of stability boundaries in a natural circulation single-phase thermosyphon loop. *Int. J. Heat Fluid Flow* 24: 853–863

[14] Desrayaud G, Fichera A and Marcoux M 2006 Numerical investigation of natural circulation in a 2D-annular closed-loop thermosyphon. *Int. J. Heat Fluid Flow* 27: 154–166

[15] Sharma M, Pilkhwal D S, Vijayan P K, Saha D and Sinha R K 2010 Steady-state and linear stability analysis of a supercritical water natural circulation loop. *Nucl. Eng. Des*. 240: 588–597

[16] Chen L, Zhang X R, Yamaguchi H and Liu Z S S 2010 Effect of heat transfer on the instabilities and transitions of supercritical CO_2 flow in a natural circulation loop. *Int. J. Heat Mass Transf.* 53: 4101–4111

[17] Nayak A K, Gartia M R and Vijayan P K 2009 Thermal–hydraulic characteristics of a single-phase natural circulation loop with water and Al_2O_3 nanofluids. *Nucl. Eng. Des*. 239: 526–540

[18] Zboray R, Kruijf W J M D, Hagen T H J J V D and Uddin R 2004 Investigating the nonlinear dynamics of natural-circulation boiling two-phase flows. *Nucl. Technol*. 146: 244–256

[19] Satoh A, Okamoto K and Madarame H 1998 Instability of single-phase natural circulation under double loop system. *Chaos Soliton Fract*. 9: 1575–1585

[20] Saha R 2013 *Experimental and Numerical Study of a Single Phase Square Natural Circulation Loop*. M. E. Thesis, School of Nuclear Studies and Application—Jadavpur University, Kolkata

[21] Saha R, Sen S, Mookherjee S, Ghosh K, Mukhopadhyay A and Sanyal D 2015 Experimental and numerical investigation of a single-phase square natural circulation loop. *J. Heat Transf.* 137: 121010-1–121010-8

[22] Li Y, Yang Y, Li G, Xu M and Huang W 2017 A fault diagnosis scheme for planetary gearboxes using modified multi-scale symbolic dynamic entropy and mRMR feature selection. *Mech. Syst. Signal Process*. 91: 295–312

[23] Mukhopadhyay A, Chaudhari R R, Paul T and Sen S 2013 Lean blow-out prediction in gas turbine combustors using symbolic time series analysis. *J. Propul. Power* 29: 950–960

[24] Ray A 2004 Symbolic dynamic analysis of complex systems for anomaly detection. *Signal Process*. 84: 1115–1130

[25] Rajagopalan V and Ray A 2006 Symbolic time series analysis via wavelet-based partitioning. *Signal Process*. 86: 3309–3320

[26] Vijayan P K, Bade M H, Saha D, Sinha R K and Raj V V 2004 A generalized flow correlation for single-phase natural circulation loops. In: *XVII National and VI ISHMT/ASME Heat and Mass Transfer Conference*. IGCAR Kalpakkam

[27] Saha R, Ghosh K, Mukhopadhyay A and Sen S 2017 Flow dynamics study of a single-phase square NCL using recurrence plot and recurrence quantification. *Indian Acad. Sci. Conf. Ser.* 1: 67–75

[28] Saha R, Ghosh K, Mukhopadhyay A and Sen S 2018 Dynamic characterization of a single-phase square natural circulation loop. *Appl. Therm. Eng*. 128: 1126–1138